High Resolution 3D Earth Observation Data Analysis for Safeguards Activities

Pablo d'Angelo[a][1]**, Cristian Rossi**[a]**, Christian Minet**[a]**, Michael Eineder**[a]**, Michael Flory**[b]**, Irmgard Niemeyer**[c]

[a] German Aerospace Research Center, Remote Sensing Technology Institute
[b] International Atomic Energy Agency (IAEA), Vienna, Austria
[c] Forschungszentrum Jülich

Abstract. This paper provides an overview of the investigations performed at DLR with respect to the application of high resolution SAR and optical data for 3D analysis in the context of Safeguards. The Research Center Jülich and the adjacent open cut mines were used as main test sites, and a comprehensive stack of ascending and descending TerraSAR data was acquired over two years. TerraSAR data acquisition was performed, and various ways to visualize and analyze stacks of radar images were evaluated. Building height estimation was performed using a combination of ascending-descending radar images, as well as height-form-shadow and height-from-layover. A tutorial on building signatures from SAR images highlighted the sensor specific imaging characteristics. These topics were particularly relevant in safeguards activity with a "small-budget" as only a single image – or a couple - were employed. Interferometric coherence map interpretation allows the detection of traffic on dirt roads. Digital surface models (DSM) were generated from TanDEM-X interferometric data and from optical VHR data. Sub-meter Worldview-2 and GeoEye-1 data was processed into highly detailed DSM with a grid spacing of 1 m, showing building structures. 3D change and volume detection was performed with both optical and radar DSMs. The TanDEM-X DSMs proved useful for volume change detection and computation in mining areas, and DSMs generated from optical satellite data show details on the building level. Virtual 3D fly-throughs were found to be a good tool to provide an intuitive understanding of site structure and might be useful for inspector briefing.

1. Introduction

The primary remote sensing datasets used for safeguards purposes are optical satellite images with a resolution from 0.5 to 1 m. Most information is obtained by visual analysis of the scenes by expert image analysts. However, optical data depends on good weather conditions and is typically acquired only in the late morning. Synthetic aperture radar (SAR) data is a complementary data source, as it provides weather independent datasets, but its unintuitive depiction of complex industrial facilities hampers visual interpretation of the data.

During a multi-year study, DLR has acquired extensive stacks of very high resolution TerraSAR-X high-resolution spotlight images over the Forschungszentrum Jülich as an example site with complex, industrial structure and adjacent mining areas. The goal of the study was to better understand SAR imagery and to develop methodologies for exploitation of SAR imagery in context of safeguards relevant applications. Besides visual interpretation, determination of 3D information such as building heights or volume change in mines and waste dumps is an important topic. In the second and third phase, generation of digital surface models (DSM) from optical satellite stereo data additionally became an interesting topic, as new matching algorithms can provide fine details not achievable with classical patch based image correlation.

---

[1] Corresponding author, pablo.angelo@dlr.de

2. SAR

2.1. TerraSAR-X and PSI processing

Since June 2007, TerraSAR-X satellite is producing high-resolution SAR satellite data in several acquisition modes [1]. High-resolution spotlight (HRS) images are taken over a specific area of about 50 km^2 with a ground resolution of less than one meter. In the cooperation between the German IAEA support programme and DLR, a stack of 39 HRS images in ascending configuration and 41 HRS images in descending configuration has been employed and various applications such as Permanent Scatterer Interferometry (PSI) and Digital Elevation Model (DEM) change detection have been exploited [1]. An exemplary result of deformation map generated with PSI is shown in Figure 1. These maps are powerful tools for the evaluation of local subsidence or local uplift and nowadays are standard products of SAR service providers and research centers like DLR.

Figure 1. PSI deformation map over FZ Jülich using the descending HRS TerraSAR-X stack.

2.2. Urban applications: building height estimation

SAR imaging of urban areas is affected by distortions such as layover, i.e. the superposition in a single resolution cell of contributions coming from different areas, and shadow, i.e. the absence of useful signal because of non-illumination. Moreover, multiple-bounces and particular urban features such as windows eaves and corners yield high reflectivity. The interpretation of SAR images is therefore complex and requires the knowledge of the system and its sensibility [2]. On the one hand, the side-looking geometry may pose difficulties to remote sensing image analysts. Nevertheless, on the other hand, it enables a set of applications as building height retrieval with just a single or a couple of images. In the following a couple of algorithms for the building height derivation are summarized.

2.2.1. Building height from shadow

This classical algorithm can be applied also to SAR images, according to the geometry in Figure 2. An example of shadow appearance in the SAR amplitude is shown at the right side. If the image is in SAR

coordinates, i.e. range and azimuth, the building height can be determined with a simple equation, once detected the shadow length Δr of a range transect: $h = \Delta r \cdot \cos(\theta)$.
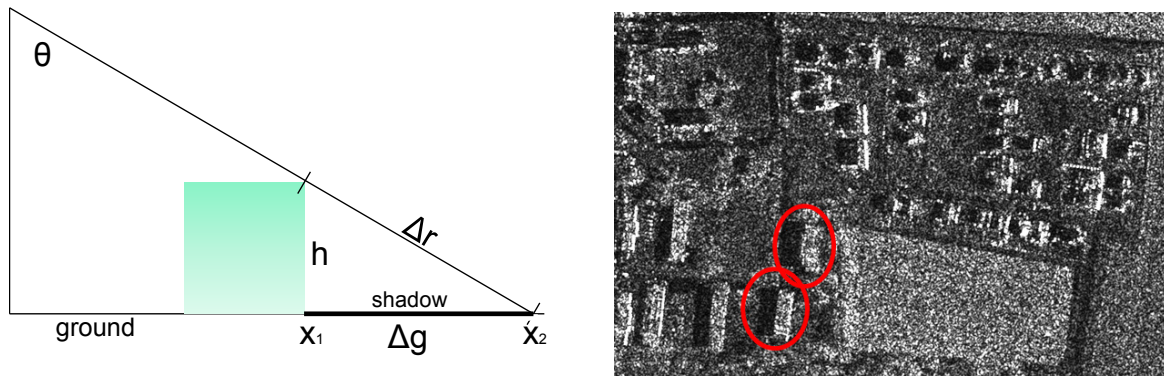

Figure 2. (left) Geometry for the computation of building height from shadow areas. (right) Example of building shadows in a SAR amplitude image.

This technique is very simple and produces a first guess of the building height. It requires only a single SAR image. The main limitation is the shadow detection, as shadow might be overlaid with layover or being in low reflectivity zone.

2.2.2. Building height from ascending/descending data fusion

This technique exploits the appearance of an object from two different geometries, i.e in ascending and descending orbits. It requires two orthorectified TerraSAR-X images (*EEC product*). The main concept is the following: the geometrical distance between a single feature is proportional to the feature height in the superposition of the two images. SAR images are othorectified by using an external DEM or a fixed terrain height. The height in which the feature under analysis is orthorectified plays a role in the feature elevation estimation, as depicted in Figure 3. In the figure, θ is the incidence angle and β the system heading angle, both derivable from the TerraSAR-X product annotation.

For this technique, an overlay of the two input images shall be firstly produced. In Figure 3, an example of RGB composite (ascending: red, descending: green+blue) for a weather tower is shown. By measuring the distances between common points, the tower height can be easily retrieved following the guidelines in Figure 4.

Actually, when the span between the top and the bottom of the feature is visible, as in Figure 4, an easier relationship can be established and a single image can be employed: $\Delta xy_1 = h / \tan(\theta_1)$.
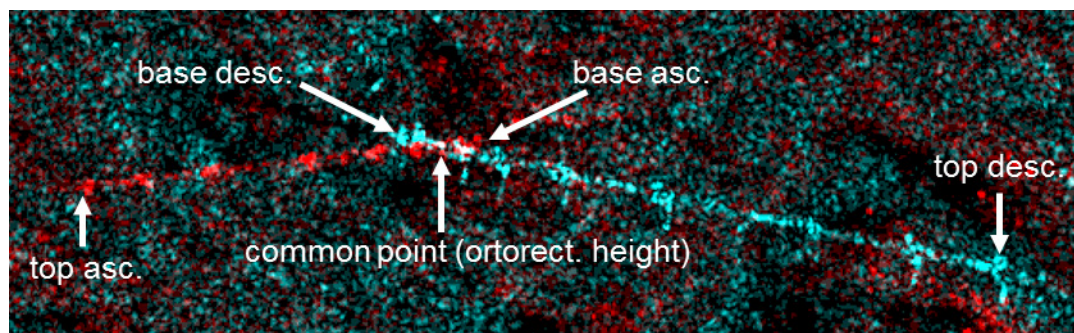

Figure 3. Example of appearance of a weather tower in a RGB composite built using two SAR images.

$$h = \frac{\Delta xy}{\sqrt{\left[\left(-\frac{1}{\tan\theta_1}\cos\beta_1 + \frac{1}{\tan\theta_2}\cos\beta_2\right)^2 + \left(\frac{1}{\tan\theta_1}\sin\beta_1 + \frac{1}{\tan\theta_2}\sin\beta_2\right)^2\right]}}$$

$$h = \frac{\left(\Delta xy_1 + \Delta xy_2\right)}{\sqrt{\left[\left(-\frac{1}{\tan\theta_1}\cos\beta_1 + \frac{1}{\tan\theta_2}\cos\beta_2\right)^2 + \left(\frac{1}{\tan\theta_1}\sin\beta_1 + \frac{1}{\tan\theta_2}\sin\beta_2\right)^2\right]}}$$

$$h = \frac{\left(\Delta xy_1 - \Delta xy_2\right)}{\sqrt{\left[\left(-\frac{1}{\tan\theta_1}\cos\beta_1 + \frac{1}{\tan\theta_2}\cos\beta_2\right)^2 + \left(\frac{1}{\tan\theta_1}\sin\beta_1 + \frac{1}{\tan\theta_2}\sin\beta_2\right)^2\right]}}$$
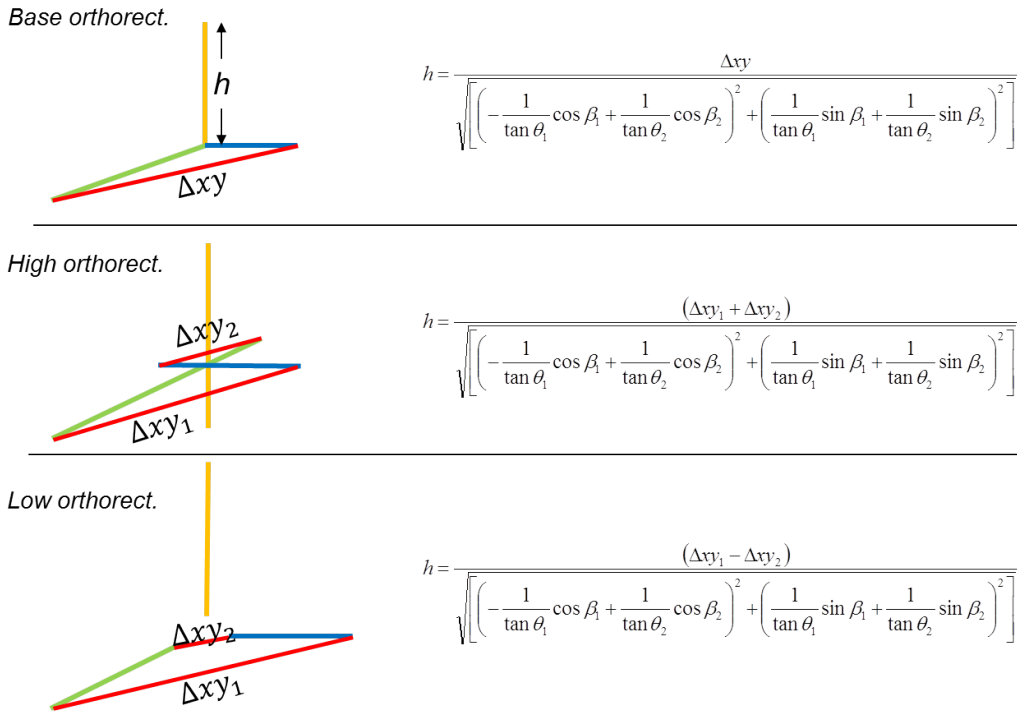
Figure 4. Computation of object elevation from two complementary SAR views. In yellow, the object is represented. In blue and green, the object as seen from the two SAR images. Three possible cases are analyzed. At the top, the SAR image is locally orthorectified on a height corresponding to the object base. At the middle, the SAR image is locally orthorectified on a higher height, while at the bottom on a lower height. In the right part, the equations for the computation of the object height are expressed. θ represents the incidence angle and β the system heading angle.

2.3. Coherent change detection: dirt roads usage
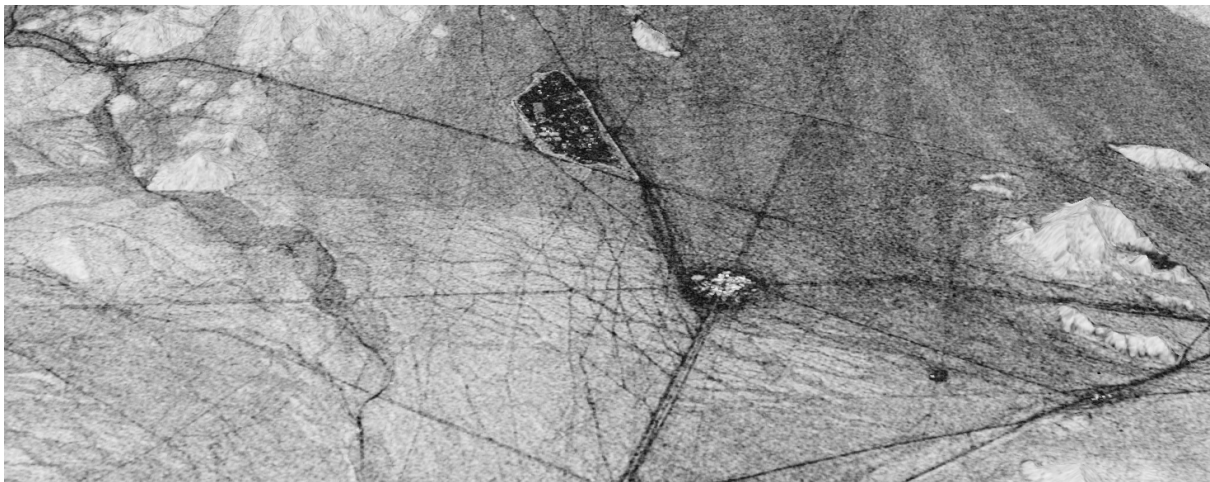

Figure 5. Detail of the coherence map in the proximity of Fort Irwin (USA) generated with two TerraSAR-X images with a temporal baseline of 11 days. The network of used roads is easily recognizable (dark tones).

Coherence is a measure of similarity between two SAR images in an interferometric scenario. The main source of correlation loss is the change of scattering in time. For instance, water surfaces show zero coherence after milliseconds. Agricultural fields show a moderate coherence after a day and low

coherence after months. Exposed rocks and urban areas show high coherence even after years. In this context, interferometric coherence can be exploited in the detection of used and unused dirt roads.

Unused dirt roads keep their structural characteristics for a long time in moderate weather conditions, showing therefore high coherence values. Contrariwise, used dirt roads lose their structural characteristics after the passage of car, trucks, tanks and etc. An analysis of the coherence map in Figure 5 allows the detection of used dirt roads within the temporal baseline of the two TerraSAR-X acquisitions. In this case, an example over Fort Irwin (USA) for a temporal baseline of 11 days is shown.

3. Optical images

In addition to radar imagery, optical images are widely employed for monitoring of safeguards relevant sides. Most safeguards relevant information can be derived with visual interpretation by image analysts. Additionally, advanced image matching techniques, together with sub-meter resolution stereo imagery can provide high resolution digital surface models (DSM) that resolve details of industrial buildings and provide a good base for monitoring of changes to buildings or excavation, dumping and mining activities.

The DSM generation process consists of two major parts: Image orientation and Image matching. Good results in industrial areas can be archived with stereo pairs with a convergence angle between 15 to 25 degrees, otherwise too many occlusions would occur. This will result in incomplete height measurements in dense building areas. For best quality, tri-stereo acquisitions with a relative convergence angle of around 15 degrees are recommended [5]. The scenes should be acquired in the same satellite pass, otherwise temporal and illumination changes can lead to incomplete DSMs.

3.1. Image orientation

Image matching and later DSM comparisons require a good relative orientation, with an accuracy of around 0.5 pixels. This can be archived using bundle block adjustment [6] of all images used for DSM generation and comparison. First, tie points are matched between all images with the SIFT [7] operator and then further refined with local least squares matching [8]. Optionally, reference information in the form of reference DEMs, reference images, or ground control points can be employed in this process, if an absolute accuracy better than the system accuracy of the used satellites is required. Without reference data, typical absolute accuracies are 4 – 6 m for WorldView and GeoEye satellites.

In practical image analysis applications, co-registration of images is often performed in a non-rigorous way, for example by ortho-rectification and later image to image registration, due to data handling issues or licencing costs of the bundle adjustment software. This process does not improve the sensor models or RPCs and thus cannot be used as part of the DSM generation workflow.

3.2. DSM generation

To resolve detailed structures, a correspondence for every pixel in the first stereo image should be found in the second image. In the last years, Semi Global Matching (SGM) [8] has proven to be a robust method that can deliver DSMs with more details than traditional window based correlation methods usually implemented in commercial off the shelf (COTS) software. For every pixel and all possibly correspondent pixels in the second image, a matching cost is computed. As the matching costs based on single pixel values or small windows are ambiguous, regularization is used to ensure a well behaved reconstruction.

3.3. Application to Forschungszentrum Jülich

The Forschungszentrum Jülich was used as a test site and two stereo pairs were available for this region: One WorldView-2 pair acquired in March 2011, and a GeoEye stereo pair acquired in October 2012. The WorldView-2 pair was processed in 2011 first, resulting in a DSM with a grid spacing of 1 m, and an ortho image. As the data was acquired during leaf-off conditions, the broad leaved forest
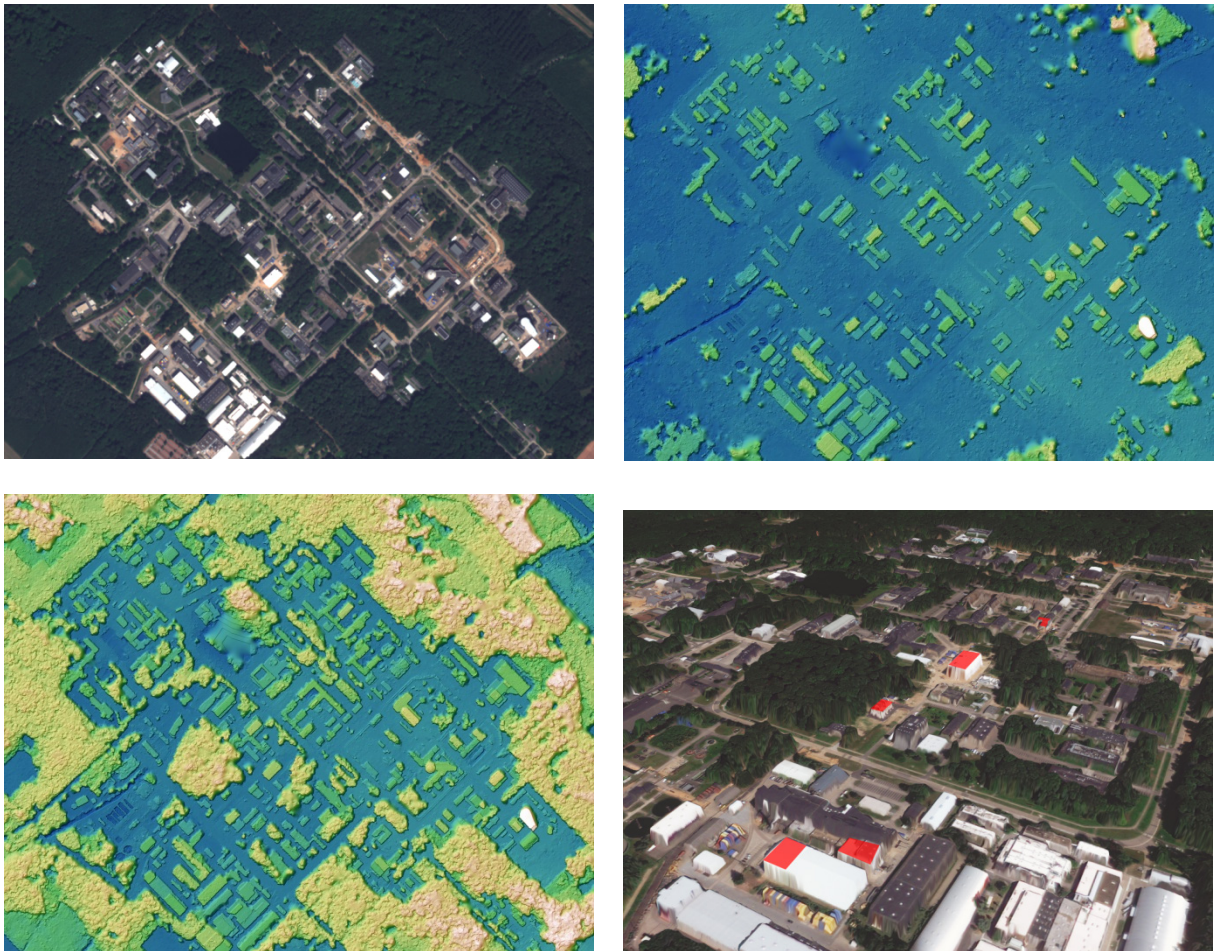
5

Figure 6: Forschungszentrum Jülich (upper left), DSMs derived from WorldView II (upper right) and GeoEye (lower left). 3D view created from GeoEye DSM and ortho image (lower right). The red areas highlight new buildings and building extension derived by 3D change detection between the 2011 and 2012 DSMs.

around the research center is not visible in the Worldview DSM. The GeoEye scene was bundle adjusted using the Worldview-2 ortho and DSM as a reference, thus both DSMs and the corresponding ortho images are perfectly aligned, and can be used for 3D change detection.

The DSMs show a high amount of details, as seen in Figure 6, and can be used measure building heights, derive the number of containers stacked on top of each other or perform 3D change detection on the building level.

3.4.   Volume change detection.

The difference of two digital elevation models yields the immediate detection of height changes. The time span in between the models defines the period in which the changes took place. For instance, when employing one TanDEM-X DEM [3] and one SRTM DEM [4], a decadal elevation change can be derived by differentiating them. The decadal earth changes can be useful for geophysical studies such as glacier analysis. Short time analysis requires shorter temporal baselines. TanDEM-X acquisitions or DSMs generated from optical stereo can be used for the purpose. An example of DEM differences is in Figure 8. The difference image shows the location and the volume of the excavations as well as the location and the volume of the accumulation. DSMs with a resolution of 5 to 30 meters, such as SRTM and TanDEM-X are useful for larger scale mining applications, while higher resolution DSMs can be used for building change detection and monitoring of smaller changes, cf. Figure 6.
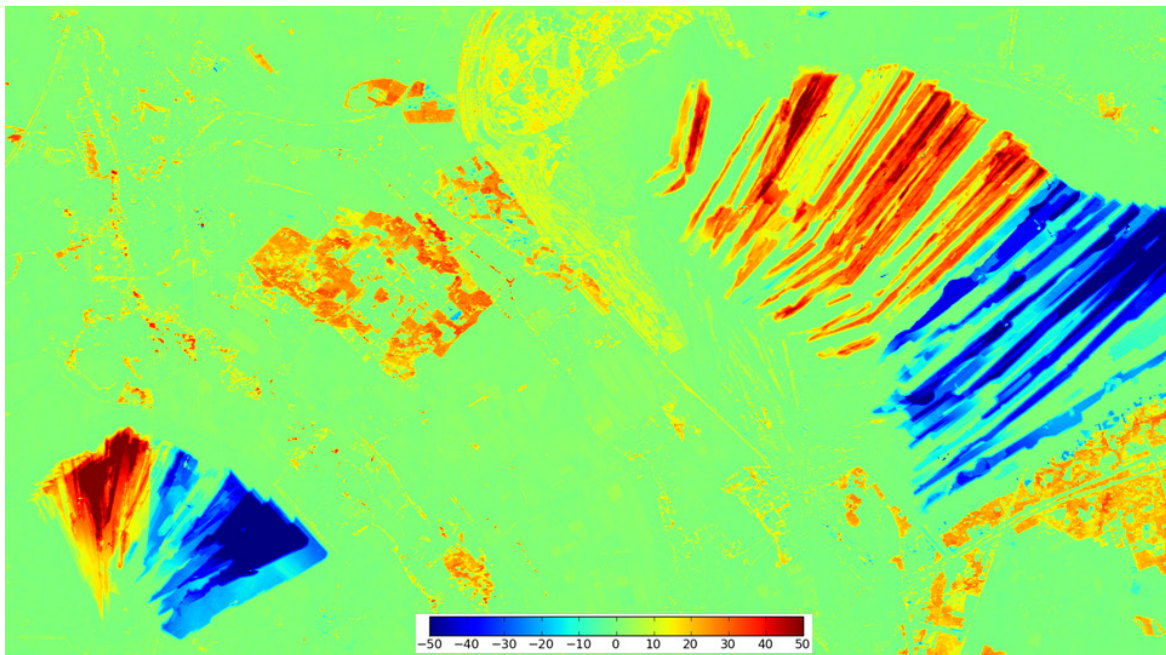
6

Figure 8: DSM difference of the Forschungszentrum Jülich between March 2011 and October 2012, the color shows height changes in meters. Accumulations are shown in red, excavations in blue. The total volume change for the Inden mine in the south west corner was -49.1 Million cubic meters.

4. Summary and conclusion

The study has shown that valuable information can be derived from SAR images, although some techniques are not readily applicable without large stacks of data, such as persistent scatterer analysis. This large amount of data is often not available, as acquisition of stacks needs to be performed over a long time period, and results in large data costs.

Therefore techniques that require only one or at most two SAR images are most relevant in a practical scenario. When understanding the building signatures and through simple geometrical constraints, building height information can be retrieved from a single image or a pair of ascending/descending TerraSAR-X high-resolution spotlight images. Coherent change detection allows the detection of used dirt roads, but requires a more involved processing. Digital elevation models can be computed by stereo matching of optical stereo pairs, or by SAR interferometry. This information is most relevant for the detection and monitoring of infrastructure and safeguard relevant processes. DSMs from TerraSAR-X interferometric pairs are suitable for mining applications, but do not allow high quality reconstruction of industrial buildings. Here, optical stereo data with a sub-meter resolution can provide the basis for 3D change detection and volume measurement of small waste dumps. Tools to perform these tasks have been provided to IAEA to facilitate an in-house analysis of relevant sites.

Future work includes improvements to the DSM generation from optical stereo data and streamlining of the data handling workflow. Additionally, in track stereo imagery is often not available due to budgetary and data collection constraints. DSM generation from stereo pairs acquired by different sensors or with different acquisition dates is being evaluated. Spaceborne video, as acquired by Skybox Imaging/Google is another interesting data source. Possible applications include DSM generation, object detection and activity monitoring.

5. Acknowledgements

6. References

[1] MINET, C., EINEDER M., REZNICZEK A.,NIEMEYER I., High Resolution Radar Satellite Imagery Analysis for Safeguards Applications, ESARDA BULLETIN, No. 46 (2011).

[2] ROSSI C., GERNHARDT S., Urban DEM generation, analysis and enhancements using TanDEM-X, ISPRS Journal of Photogrammetry and Remote Sensing 85 (2013), pp. 120-131.

[3] KRIEGER G., ET AL., TanDEM-X: a satellite formation for high-resolution SAR interferometry, IEEE TGRS, (2007).

[4] RABUS, B., EINEDER M., ROTH A., BAMLER R., The shuttle radar topography mission- a new class of digital elevation models acquired by spaceborne radar, Photogramm. Rem. Sens., v. 57 (2003), pp. 241-262.

[5] CARL, S., BÄRISCH, S., LANG, F., D'ANGELO, P., AREFI, H.,REINARTZ, P, Operation Generation of High Resolution Digital Surface Models from Commercial Tri-Stereo Satellite Data, Photogrammetric Week 2013, pp. 261-269.

[6] GRODECKI, J. AND DIAL, G., Block Adjustment of High-Resolution Satellite Images Described by Rational Functions. Photogrammetric Engineering and Remote Sensing 69(1), (2003), pp. 59–70.

[8] LOWE, D.G., Distinctive image features from scale-invariant keypoints. International Journal of Computer Vision, 60 (2), (2004), pp. 91-110.

[9] ACKERMANN, F., 1983 High Precision Digital Image Correlation. Proceedings of 39th Photogrammetry Week, University of Stuttgart (1983), pp. 231-243.